Physics Letters B 772 (2017) 483–488

Contents lists available at ScienceDirect

Physics Letters B

www.elsevier.com/locate/physletb

Observation of a γ-decaying millisecond isomeric state in $^{128}Cd_{80}$

A. Jungclaus [a,*], H. Grawe [b], S. Nishimura [c], P. Doornenbal [c], G. Lorusso [c], G.S. Simpson [d], P.-A. Söderström [c], T. Sumikama [e], J. Taprogge [a,f,c], Z.Y. Xu [c], H. Baba [c], F. Browne [h,c], N. Fukuda [c], R. Gernhäuser [i], G. Gey [d,j,c], N. Inabe [c], T. Isobe [c], H.S. Jung [k,1], D. Kameda [c], G.D. Kim [l], Y.-K. Kim [l,m], I. Kojouharov [b], T. Kubo [c], N. Kurz [b], Y.K. Kwon [l], Z. Li [n], H. Sakurai [c,g], H. Schaffner [b], Y. Shimizu [c], K. Steiger [i], H. Suzuki [c], H. Takeda [c], Zs. Vajta [o,c], H. Watanabe [c], J. Wu [n,c], A. Yagi [p], K. Yoshinaga [q], G. Benzoni [r], S. Bönig [s], K.Y. Chae [t], L. Coraggio [u], J.-M. Daugas [v], F. Drouet [d], A. Gadea [w], A. Gargano [u], S. Ilieva [s], N. Itaco [u,x], F.G. Kondev [y], T. Kröll [s], G.J. Lane [z], A. Montaner-Pizá [w], K. Moschner [aa], D. Mücher [s], F. Naqvi [ab], M. Niikura [g], H. Nishibata [p], A. Odahara [p], R. Orlandi [ac,ad], Z. Patel [ae], Zs. Podolyák [ae], A. Wendt [aa]

[a] *Instituto de Estructura de la Materia, CSIC, E-28006 Madrid, Spain*
[b] *GSI Helmholtzzentrum für Schwerionenforschung GmbH, 64291 Darmstadt, Germany*
[c] *RIKEN Nishina Center, RIKEN, 2-1 Hirosawa, Wako-shi, Saitama 351-0198, Japan*
[d] *LPSC, Université Joseph Fourier Grenoble 1, CNRS/IN2P3, Institut National Polytechnique de Grenoble, F-38026 Grenoble Cedex, France*
[e] *Department of Physics, Tohoku University, Aoba, Sendai, Miyagi 980-8578, Japan*
[f] *Departamento de Física Teórica, Universidad Autónoma de Madrid, E-28049 Madrid, Spain*
[g] *Department of Physics, University of Tokyo, Hongo 7-3-1, Bunkyo-ku, 113-0033 Tokyo, Japan*
[h] *School of Computing, Engineering and Mathematics, University of Brighton, Brighton BN2 4GJ, United Kingdom*
[i] *Physik Department E12, Technische Universität München, D-85748 Garching, Germany*
[j] *Institut Laue-Langevin, B.P. 156, F-38042 Grenoble Cedex 9, France*
[k] *Department of Physics, Chung-Ang University, Seoul 156-756, Republic of Korea*
[l] *Rare Isotope Science Project, Institute for Basic Science, Daejeon 305-811, Republic of Korea*
[m] *Department of Nuclear Engineering, Hanyang University, Seoul 133-791, Republic of Korea*
[n] *School of Physics and State Key Laboratory of Nuclear Physics and Technology, Peking University, Beijing 100871, China*
[o] *MTA Atomki, P.O. Box 51, Debrecen H-4001, Hungary*
[p] *Department of Physics, Osaka University, Machikaneyama-machi 1-1, Osaka 560-0043 Toyonaka, Japan*
[q] *Department of Physics, Faculty of Science and Technology, Tokyo University of Science, 2641 Yamazaki, Noda, Chiba, Japan*
[r] *INFN, Sezione di Milano, via Celoria 16, I-20133 Milano, Italy*
[s] *Institut für Kernphysik, Technische Universität Darmstadt, D-64289 Darmstadt, Germany*
[t] *Department of Physics, Sungkyunkwan University, Suwon 440-746, Republic of Korea*
[u] *Istituto Nazionale di Fisica Nucleare, Complesso Universitario di Monte S. Angelo, I-80126 Napoli, Italy*
[v] *CEA, DAM, DIF, 91297 Arpajon cedex, France*
[w] *Instituto de F'sica Corpuscular, CSIC-Univ. of Valencia, E-46980 Paterna, Spain*
[x] *Seconda Universita di Napoli, Dipartimento di Matematica e Fisica, 2-81100 Caserta, Italy*
[y] *Nuclear Engineering Division, Argonne National Laboratory, Argonne, IL 60439, USA*
[z] *Department of Nuclear Physics, Research School of Physical Sciences and Engineering, Australian National University, Canberra, ACT 0200, Australia*
[aa] *IKP, University of Cologne, D-50937 Cologne, Germany*
[ab] *Wright Nuclear Structure Laboratory, Yale University, New Haven, CT 06520-8120, USA*
[ac] *Instituut voor Kern- en StralingsFysica, K.U. Leuven, B-3001 Heverlee, Belgium*
[ad] *Advanced Science Research Center, Japan Atomic Energy Agency, Tokai, Ibaraki, 319-1195, Japan*
[ae] *Department of Physics, University of Surrey, Guildford GU2 7XH, United Kingdom*

* Corresponding author.
E-mail address: andrea.jungclaus@csic.es (A. Jungclaus).
[1] Present address: Department of Physics, University of Notre Dame, Notre Dame, Indiana 46556, USA.

http://dx.doi.org/10.1016/j.physletb.2017.07.006
0370-2693/© 2017 The Author(s). Published by Elsevier B.V. This is an open access article under the CC BY license (http://creativecommons.org/licenses/by/4.0/). Funded by SCOAP[3].

ARTICLE INFO

Article history:
Received 24 May 2017
Received in revised form 3 July 2017
Accepted 4 July 2017
Available online 12 July 2017
Editor: V. Metag

Keywords:
Isomeric decays
Shell model calculations
Transition strengths

ABSTRACT

A new high-spin isomer in the neutron-rich nucleus ^{128}Cd was populated in the projectile fission of a ^{238}U beam at the Radioactive Isotope Beam Factory at RIKEN. A half-life of $T_{1/2} = 6.3(8)$ ms was measured for the new state which was tentatively assigned a spin/parity of (15^-). The experimental results are compared to shell model calculations performed using state-of-the-art realistic effective interactions and to the neighbouring nucleus ^{129}Cd. In the present experiment no evidence was found for the decay of a 18^+ $E6$ spin-trap isomer, based on the complete alignment of the two-neutron and two-proton holes in the $0h_{11/2}$ and the $0g_{9/2}$ orbit, respectively, which is predicted to exist by the shell model.

© 2017 The Author(s). Published by Elsevier B.V. This is an open access article under the CC BY license (http://creativecommons.org/licenses/by/4.0/). Funded by SCOAP^3.

The regions in the nuclear chart around doubly-magic nuclei such as ^{100}Sn and ^{132}Sn offer a rich testing ground for the study of isomeric states of different types. Seniority isomers are observed due to the properties of the isovector pairing interaction which lead to a decreasing energy spacing between the excited states formed by the successive alignment of two identical nucleons occupying the same orbital. As a consequence the fully aligned state of such a two-nucleon configuration is often long-lived due to the small transition energy for the electromagnetic decay. Examples of such seniority isomers with half-lives in the µs range are the 8^+ states in the semi-magic two-proton hole nuclei ^{98}Cd$_{50}$ and ^{130}Cd$_{82}$ [1,2]. An analogous isomer based on the fully-aligned $\nu(0h_{11/2}^{-2})$, 10^+ neutron configuration is observed in the semi-magic two-neutron hole nucleus ^{130}Sn [3]. Another type of isomer frequently observed in the regions around ^{100}Sn and ^{132}Sn are spin-gap isomers. In these cases the decay to states at lower excitation energy requires a large change in nuclear spin and therefore the emission of γ rays with high multipolarity. In cases of large hindrances a decay mediated by the weak interaction, i.e. β decay, is favoured as compared to the electromagnetic decay. Examples are low-lying β-decaying states in odd nuclei around the doubly-magic Sn cores due to the closely lying $0g_{9/2}$–$1p_{1/2}$ proton and $1d_{3/2}$–$0h_{11/2}$ neutron single-particle orbitals which would require electromagnetic decays with a multipolarity of $M4$. Another example of a spin-gap isomer has recently been reported in the two-proton hole and two-neutron hole nucleus ^{96}Cd [4,5]. The observed β-decaying state with a half-life of $T_{1/2} = 0.45^{+0.05}_{-0.04}$ s was interpreted as being based on the configuration in which the two neutron holes and the two proton holes, all occupying the $0g_{9/2}$ orbit, couple to the maximum possible spin of $I = 16$. Shell-model (SM) calculations suggest that this 16^+ state lies below the 12^+ and 14^+ levels so that a γ decay would have to proceed via an $E6$ transition to the 10^+ state. Instead, β decay to the 15^+ isomeric state in ^{96}Ag as well as β-delayed proton emission populating high-spin states in ^{95}Pd have been observed [4,5].

In ^{128}Cd, containing two neutron holes and two proton holes with respect to ^{132}Sn, the observation of a 10^+ isomer ($T_{1/2} = 3.56(6)$ µs) at an excitation energy of 2.714 MeV was reported in Ref. [6] and assigned to have a predominant $0h_{11/2}^{-2}$ neutron character. SM calculations predict in addition the existence of a spin-gap isomer based on the fully aligned $\pi(0g_{9/2}^{-2})\nu(0h_{11/2}^{-2})$ configuration with a spin of 18^+, in analogy to the 16^+ isomer in ^{96}Cd. Furthermore, the recent identification of a $(21/2^+)$ γ-decaying ms isomer in the neighbouring nucleus ^{129}Cd with a dominant $\pi(0g_{9/2}^{-1}(1p, 0f_{5/2})^{-1})$ $\nu(0h_{11/2}^{-1})$ configuration [7] may suggest the existence of an analogous 15^- isomer in the even–even ^{128}Cd built on the $\pi(0g_{9/2}^{-1}(1p, 0f_{5/2})^{-1})$ $\nu(0h_{11/2}^{-2})$ configuration. It was therefore the aim of the present work to search for additional β- or γ-decaying isomers at higher angular momentum in ^{128}Cd.

The experiment was performed at the Radioactive Isotope Beam Factory (RIBF) of the RIKEN Nishina Center within the EURICA campaign. The neutron-rich ^{128}Cd nuclei were produced following the projectile fission of a 345 MeV/u ^{238}U beam with an average intensity of about 8 pnA, impinging on a 3 mm thick Be target. The ions of interest were separated from other reaction products and identified on an ion-by-ion basis by the BigRIPS in-flight separator [8]. The particle identification was performed using the ΔE-TOF-$B\rho$ method in which the energy loss (ΔE), time of flight (TOF) and magnetic rigidity ($B\rho$) are measured and used to determine the atomic number, Z, and the mass-to-charge ratio, A/q, of the fragments. Details about the identification procedure can be found in Ref. [9]. In total about 6×10^5 ^{128}Cd ions were identified, transported through the ZeroDegree spectrometer (ZDS) and finally implanted into the WAS3ABi (Wide-range Active Silicon Strip Stopper Array for β and ion detection) Si array positioned at the focal plane of the ZDS. The WAS3ABi detector [10,11] consists of eight closely packed DSSSD with an area of 60×40 mm^2, a thickness of 1 mm and a segmentation of 40 horizontal and 60 vertical strips each. All decay events detected in WAS3ABi during the first five seconds following a valid implantation signal were stored and correlated offline in space and time with the implanted ions. To detect γ radiation emitted in the decay of the implanted radioactive nuclei 12 large-volume Ge Cluster detectors [12] from the former EUROBALL spectrometer [13] were arranged in a close geometry around the WAS3ABi detector.

In a first step, spectra of γ rays observed in prompt coincidence with the first decay event after the implantation of a ^{128}Cd ion in WAS3ABi were studied applying different time windows between the implantation and the decay as well as different conditions with respect to the spatial correlation. No new γ transitions were observed besides the ones already known to occur following the decay of the ground state of ^{128}Cd [14]. Furthermore, during the analysis of the time distribution of the decay events with respect to the implantation, both with and without requiring a coincidence with one of the observed γ rays in the daughter nucleus, no indication for the existence of a second β-decaying state besides the ground state ($T_{1/2} = 245(5)$ respectively 246.2(21) ms [15,16]) was obtained. To search for a γ-decaying isomer with a half-life in the ms range we followed the procedure already successfully applied in the identification of a $(21/2^+)$, $T_{1/2} = 3.6(2)$ ms isomer in ^{129}Cd [7]. Fig. 1 shows the spectrum of γ rays detected in the Ge detectors in the time interval of -4 µs $< (t_\gamma - t_{decay}) < 20$ µs with respect to the first decay event after the implantation of a ^{128}Cd ion. Only decay events registered during the first 20 ms after the implantation were considered and furthermore they had to fulfil the condition that energy was deposited exclusively in the Si detector in which the ion was implanted. This condition was shown in Ref. [7] to significantly suppress the β-decay events and enhance those in which the emission of conversion electrons occurs.

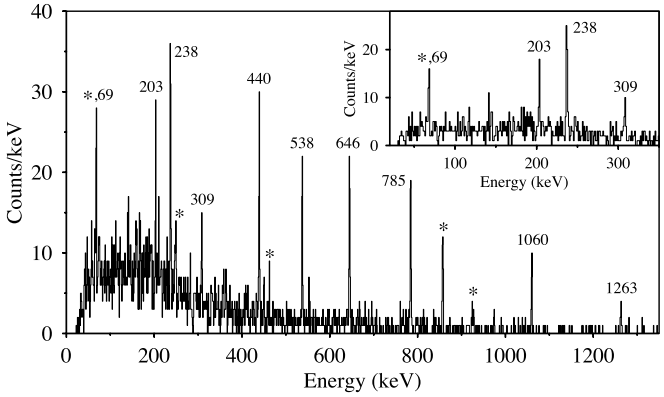

Fig. 1. Spectrum of γ rays detected in the time interval of $-4\ \mu s < (t_\gamma - t_{decay}) < 20\ \mu s$ with respect to the first decay event registered during the first 20 ms after the implantation of a ^{128}Cd ion. Only those decay events are considered in which energy was deposited exclusively in the Si detector in which the ion was implanted with an upper limit of 360 keV. Lines labelled with an asterisk correspond to known transitions in ^{128}In populated in the β decay of ^{128}Cd [14]. The inset shows the low-energy region with the strictest condition that energy was deposited exclusively in the implantation pixel.

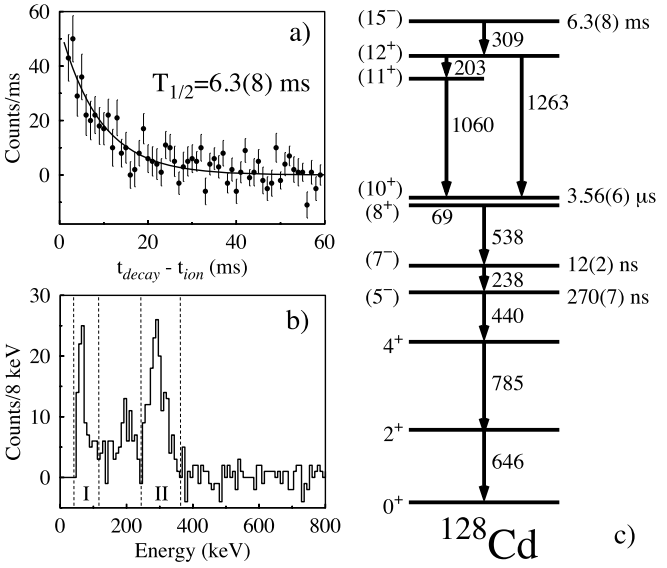

Fig. 2. a) Summed time difference distribution $(t_{decay} - t_{ion})$ for those decay events, in which one of the γ rays with energies of 203, 238, 309, 440, 538, 646, 785, 1060 and 1263 keV was detected in EURICA in the time range $-4\ \mu s < (t_\gamma - t_{decay}) < 20\ \mu s$ with respect to the decay, b) energy spectrum of decay events registered in the Si detectors in the first 20 ms after the implantation of a ^{128}Cd ion in coincidence with one of the γ rays listed above and c) proposed decay scheme of the newly established ms isomer in ^{128}Cd. The level and half-life information up to the (10^+) state is taken from Ref. [6]. Additional weak decay branches reported in [6] are omitted for simplicity.

In addition, an upper limit of 360 keV for the energy deposited in the Si detector was applied. Inspection of this spectrum shows that the γ rays with energies of 68, 248, 463, 857, and 925 keV, which are known [14] to be emitted following the β decay of ^{128}Cd to ^{128}In, are still present. However, the strongest lines at energies of 69 (part of the doublet), 238, 440, 538, 646, and 785 keV correspond to the γ rays which form the main decay sequence of the known (10^+) isomeric state at an excitation energy of 2714 keV in ^{128}Cd which has a half-life of $T_{1/2} = 3.56(6)$ µs [6]. This half-life in the microsecond range is much too short to allow for the observation of these γ rays following a direct population of this state since the dead time after each implantation amounts to one to two milliseconds. It can therefore be concluded that the (10^+) state must be populated from a new isomeric state with a half-life of at least a couple of milliseconds. In Fig. 1 four additional transitions with energies of 203, 309, 1060, and 1263 keV are clearly visible. It can be assumed that these transitions are involved in the decay of the new isomeric state to the known (10^+) microsecond isomer. The inset of Fig. 1 shows the low-energy region of the spectrum applying the additional condition that in the decay event energy was released exclusively in the pixel of the Si detector in which the ion was implanted before. This condition is the strictest one which can be applied in order to reduce contaminations and is used to demonstrate that no additional low-energy transitions can be unequivocally assigned to the decay of the new isomeric state in ^{128}Cd.

To determine the half-life of the new isomer the distribution of the time differences between the ion implantation, t_{ion}, and the detection of the decay, t_{decay}, was examined for all those decays, in which one of the γ rays with energies of 203, 238, 309, 440, 538, 646, 785, 1060, and 1263 keV was detected in the Ge array in the time range $-4\ \mu s < (t_\gamma - t_{decay}) < 20\ \mu s$ with respect to the decay. Such a wide time window rather than a prompt coincidence had to be considered due to the µs half-life of the (10^+) state ($T_{1/2} = 3.56(6)$ µs). The summed time difference distribution $(t_{decay} - t_{ion})$ is shown in Fig. 2a). A fit to the experimental points assuming a single exponential decay results in a half-life of $T_{1/2} = 6.3(8)$ ms.

In the next step, the Si energy spectrum observed in coincidence with the detection of one of the above listed γ rays was constructed for all decay events which occurred in the first 20 ms after the ion implantation. Again a time range of $-4\ \mu s < (t_\gamma - t_{decay}) < 20\ \mu s$ was considered for the γ rays. The resulting spectrum, which is displayed in Fig. 2b), reflects the distribution of energies released in the decay of the new ms isomer. Three peaks at energies around 65, 205, and 290 keV are visible in this spectrum. Based on the experience gained in the study of the decay of the ms isomer in ^{129}Cd [7] we interpret these peaks as originating from the detection of conversion electrons corresponding to the partially converted 69, 203, 238, and 309 keV transitions. As discussed in detail in our previous work, in some cases the X rays following the emission of the internal conversion electrons escape detection leading to shifts in the position of the peaks observed in the Si energy spectrum. Furthermore the energy calibration of the individual strips of the Si detectors, which has been performed using Compton scattering of the 1173 and 1333 keV γ rays emitted from a ^{60}Co calibration source, is less reliable in the low-energy regime. The 69 keV $(10^+) \rightarrow (8^+)$ $E2$ transition has an internal conversion coefficient of $\alpha(69\ \text{keV}) = 5.9$ and thus proceeds in 85% of all cases via the emission of a conversion electron (CE). However, the detection of this CE is strongly suppressed by the thresholds of the individual Si strips which in the current experiment scatter in the range 50–150 keV. Consequently only a small fraction of all 69 keV CEs, roughly one-tenth, is detected.

The sum of the newly observed 203 and 1060 keV γ rays is equal to the energy of another new transition, namely the one with 1263 keV. This observation suggests that the former two transitions form a cascade parallel to the 1263 keV γ ray. In this case the multipolarity of the 203 keV γ ray can be assumed to be rather low, most probably $M1$, which would imply a conversion coefficient of $\alpha(203\ \text{keV}) = 0.066$ for this transition. The peak areas observed in Fig. 2b) seem to indicate a larger conversion coefficient for the 309 keV transition and thus multipolarity $E3$ or higher. In the case of $E3$ the conversion coefficient would be $\alpha(309\ \text{keV}) = 0.111$. The higher multipolarity of the 309 keV transition suggests that this transition is the primary isomeric decay leading to a tentative decay sequence for the new ms isomer at an excitation energy of 4286 keV as sketched in Fig. 2c). An indirect

Table 1
Energies and relative intensities of γ rays (without correction for internal conversion) observed in the decay of the ms isomer in ^{128}Cd. In the last column estimates based on trigger probabilities and time constraints are quoted for comparison (see Appendix for details).

E_γ (keV)	E_i (keV)	I_{rel} (%)	I_{est} (%)
203	3977	40(7)	35
238	2108	85(10)	81
309	4286	38(7)	37
440	1871	87(12)	100
538	2646	78(12)	100
646	646	100(14)	100
785	1430	105(15)	100
1060	3774	52(12)	47
1263	3977	28(9)	28

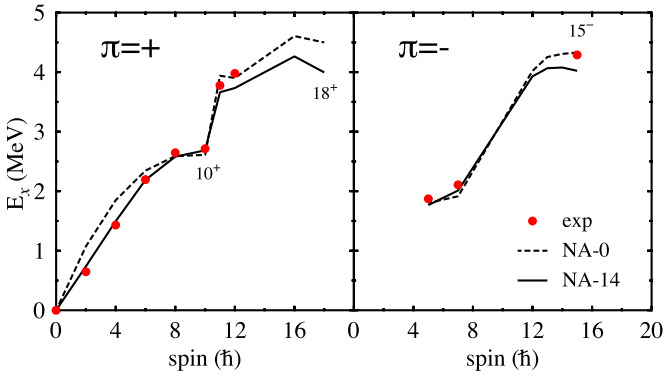

Fig. 3. Comparison between the experimental excitation energies (red dots) and those obtained by the SM calculations using the NA-0 (dashed line) and NA-14 (solid line) interactions. (For interpretation of the references to colour in this figure legend, the reader is referred to the web version of this article.)

check of the scenario proposed in Fig. 2c) is provided by a comparison of the γ-ray intensities following the decay of the (15^-) isomer expected on the basis of the experimental trigger conditions to the experimentally observed ones. This comparison, which is summarized in Table 1 and discussed in detail in the Appendix, shows that the proposed decay sequence is in full agreement with the experimental observations.

In the following we will compare the excited states of ^{128}Cd shown in Fig. 2c) to two different SM calculations. The first, named NA-0 in the following, employs a two-body effective interaction derived from the CD-Bonn nucleon–nucleon potential renormalized by way of the V_{low-k} approach [17]. Specifically, the interaction is constructed by assuming ^{132}Sn as closed core and considering the full $N = 50$–82 major shell for neutrons (i.e. the $0g_{7/2}$, $1d_{5/2}$, $1d_{3/2}$, $2s_{1/2}$ and $0h_{11/2}$ orbitals) and the $Z = 28$–50 shell for protons (i.e. the $0f_{5/2}$, $1p_{3/2}$, $1p_{1/2}$ and $0g_{9/2}$ orbits). The neutron single-particle energies (SPE) were taken from Ref. [18], while for the protons energies of 0.365 $(1p_{1/2})$ and 1.353 MeV $(1p_{3/2})$ relative to the $0g_{9/2}$ orbital were employed [19,20]. For the experimentally still unknown energy of the $0f_{5/2}$ proton orbital a value of 2.6 MeV relative to $0g_{9/2}$ was adopted. Note that these calculations are similar to the ones presented for ^{128}Cd in Refs. [21,22] in which, however, slightly different SPE have been employed. This and all following calculations were performed with the code OXBASH [23].

An inspection of Fig. 3 shows that with the NA-0 interaction the 2^+, 4^+, and 6^+ states are calculated too high in energy. This is particularly true for the 2^+ state, whose anomalously low excitation energy was traced back in Ref. [24] to special characteristics of the Cd isotopes which favour prolate configurations close to the N = 82 shell closure. Furthermore, the 15^- level is positioned

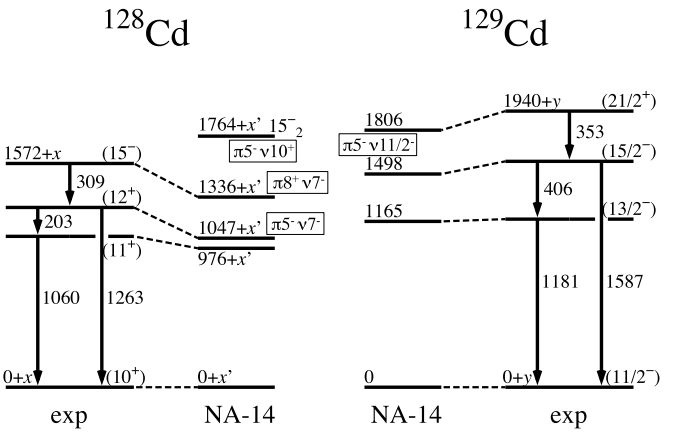

Fig. 4. Comparison between the level structures on top of the (10^+) isomer in ^{128}Cd and above the $(11/2^-)$ level in ^{129}Cd with the corresponding shell-model calculations employing the NA-14 interaction. The states in ^{128}Cd have been shifted to align the (10^+) level with the $(11/2^-)$ state in ^{129}Cd ($x = 2714$ keV, $x' = 2686$ keV). Note that it is presently experimentally unknown which of the two β-decaying states of ^{129}Cd, $3/2^+$ or $11/2^-$, is the ground state (i.e. y is unknown).

above the 13^- and 14^- states and consequently the experimentally observed isomeric character of this state is not reproduced by the NA-0 calculations. In our recent studies of several neutron-rich Cd and In isotopes a modified interaction named NA-14 was proposed which was shown to cure some of the shortcomings of NA-0 and to provide a consistent description of $46 \leq Z \leq 50$, $N \leq 82$ nuclei [7,25–27]. The modifications concerned the pairing and multipole parts of the interaction, in particular the $\pi\pi$ pairing was reduced to 88% and the $\nu\nu$ and $\pi\nu$ multipoles were increased by factors of 1.6 and 1.5 in the dominant configurations $\nu(0h_{11/2}^{-2})$ and $\nu(0h_{11/2})\pi(0g_{9/2})$. As shown in Fig. 3, the calculations employing NA-14 describe much better the level sequence up to the (10^+) isomer and also reproduce the isomeric character of the 15^- state. However, in contrast to the NA-0 calculations, they exhibit a clear overbinding of all states above the 10^+ isomer and in addition the experimental $E2/M1$ branching ratio of roughly 40/60% for the decay of the (12^+) state is badly reproduced by the NA-14 calculations (84/16%). As a last comment on Fig. 3, we would like to point out that a 18^+ $E6$ spin-gap isomer is robustly predicted by both calculations and its observation therefore remains a challenge for future experiments.

As mentioned in the introduction, recently the decay of a $(21/2^+)$ γ-decaying ms isomer with the dominant $\pi(0g_{9/2}^{-1}(1p, 0f_{5/2})^{-1})$ $\nu(0h_{11/2}^{-1})$ configuration was observed in the neighbouring nucleus ^{129}Cd [7] and interpreted as stretched coupling between the neutron hole in the $0h_{11/2}$ orbit and the 5^- proton state in semi-magic ^{130}Cd. One obvious possibility would therefore be that the (15^-) state in ^{128}Cd is formed by the analogous fully aligned $\pi(0g_{9/2}^{-1}(1p, 0f_{5/2})^{-1})$ $\nu(0h_{11/2}^{-2})$ configuration (in the following abbreviated $\pi 5^-\nu 10^+$). As illustrated in Fig. 4, the level structures observed in the decays of the (15^-) level in ^{128}Cd and the $(21/2^+)$ state in ^{129}Cd are indeed very similar. Both isomers decay via an $E3$ transition followed by parallel $M1$ and $E2$ decay branches. Note, however, that the level sequence in ^{129}Cd is much more stretched as compared to the one above the (10^+) level in ^{128}Cd, leading to a difference of more than 350 keV between the (15^-) and $(21/2^+)$ levels relative to the (10^+) and $(11/2^-)$ neutron states, respectively (compare Fig. 4). Since ^{128}Cd has both two proton and two neutron holes with respect to ^{132}Sn, there is of course a natural alternative to the $\pi 5^-\nu 10^+$ configuration for the 15^- state, namely the stretched coupling between the $\pi(0g_{9/2}^{-2})$

Table 2
Experimental and calculated (NA-14) $B(E3)$ values in W.u. for transitions in ^{128,129}Cd and ^{129}In.

Nucleus	I_i^π	I_f^π	$B(E3)_{exp}$ (W.u.)	$B(E3)_{SM}$ (W.u.)
^{128}Cd	(15^-)	(12^+)	0.66(8)	0.42
^{129}Cd	$(21/2^+)$	$(15/2^-)$	0.47(3)[1]	0.46
^{129}In	$(29/2^+)$	$(23/2^-)$	0.069(10)	0.042

[1] Note that in Ref. [7], by mistake, a slightly larger value of $B(E3) = 0.50(3)$ W.u. was quoted due to the omission of taking into account the internal conversion coefficient $\alpha = 0.0665$ [29] of the 353 keV $E3$ transition.

and the $\nu(0h_{11/2}^{-1}1d_{3/2}^{-1})$ configurations ($\pi 8^+\nu 7^-$), i.e. the known 8^+ and 7^- isomers in the respective two-proton and two-neutron hole nuclei ^{130}Cd and ^{130}Sn.

An inspection of the wave functions obtained using the NA-type interactions shows that the leading configuration of the yrast 15^- state is indeed robustly $\pi 8^+\nu 7^-$, while the second 15^- state, which is predicted 330–530 keV higher in energy, is dominated by the $\pi 5^-\nu 10^+$ configuration. Note that the calculated energy of this second 15^- relative to the 10^+ state nicely agrees with the energy of the $\pi 5^-\nu(0h_{11/2}^{-1})$, $21/2^+$ state in ^{129}Cd. In the odd-Z, two-neutron hole nucleus ^{129}In isomeric states with spins of $(23/2^-)$ and $(29/2^+)$ have been observed at excitation energies of 1630(56) and 1911(56) keV, respectively [28]. The energies of these states, which are based on the stretched $\pi(0g_{9/2}^{-1})\nu 7^-$ and $\pi(0g_{9/2}^{-1})\nu 10^+$ configurations, are calculated only about ∼100 keV lower by the shell model employing the NA-14 interaction. Turning now to the transition probabilities it is worth mentioning that the strength of all three $E3$ transitions discussed above, namely the $(15^-) \rightarrow (12^+)$ in ^{128}Cd, the $(21/2^+) \rightarrow (15/2^-)$ in ^{129}Cd and the $(29/2^+) \rightarrow (23/2^-)$ in ^{129}In, are well reproduced by the current calculations (see Table 2) using effective charges of $e_\pi = 1.5e$ and $e_\nu = 0.7e$.

Finally, we can now use the NA-14 interaction to predict the positions of the remaining excited states in $^{128\text{–}130}$Cd which are based on fully aligned configurations and have not yet been fixed experimentally. The $\pi 8^+\nu(0h_{11/2}^{-1})$, $27/2^-$ state in ^{129}Cd is calculated at an energy of 1695 keV, while the $\pi(0g_{9/2}^{-1}(1p, 0f_{5/2})^{-1})$, 5^- level in ^{130}Cd is predicted at an energy of 2075 keV, 27 keV below the calculated energy of the 8^+ state. Finally, the seniority $\upsilon = 4, 18^+$ spin-gap isomer in ^{128}Cd is predicted to have an excitation energy of 3995 keV.

To conclude we reported on the identification of a new isomeric state with a half-life of $T_{1/2} = 6.3(8)$ ms in the nucleus ^{128}Cd which decays via the emission of a γ ray with an energy of 309 keV and a multipolarity $E3$. The decay was identified via the observation of known γ rays emitted following the decay of the (10^+) isomeric state in coincidence with the detection of internal conversion electrons in an active stopper. Based on the observed γ-ray intensities and state-of-the-art shell model calculations we tentatively assigned a spin/parity of 15^- to this state. The shell-model study of ^{128}Cd presented here reinforces the conclusions from our previous work that adjustments of the pairing and multipole parts of the effective interaction derived from the CD-Bonn nucleon–nucleon potential are required in order to describe the properties of nuclei in the region around ^{132}Sn. Finally, predictions are made for the excitation energies of the still unobserved $27/2^-$ state in ^{129}Cd, the 5^- level in ^{130}Cd, and the 18^+ spin-gap isomer in ^{128}Cd.

Acknowledgements

We thank the staff of the RIKEN Nishina Center accelerator complex for providing stable beams with high intensities to the experiment. We acknowledge the EUROBALL Owners Committee for the loan of germanium detectors and the PreSpec Collaboration for the readout electronics of the cluster detectors. This work was supported by the Spanish Ministerio de Ciencia e Innovación under contract FPA2011-29854-C04 and the Spanish Ministerio de Economía y Competitividad under contract FPA2014-57196-C5-4-P, the Generalitat Valenciana (Spain) under grant PROMETEO/2010/101, the National Research Foundation of Korea (NRF) grant funded by the Korea government (MEST) (NRF-2014S1A2A2028636, 2016K1A3A7A09005579, 2016R1A5A1013277), the Priority Centers Research Program in Korea (2009-0093817), OTKA contract number K-100835, JSPS KAKENHI (Grant No. 25247045), the European Commission through the Marie Curie Actions call FP7-PEOPLE-2011-IEF under Contract No. 300096, the U.S. Department of Energy, Office of Nuclear Physics, under Contract No. DE-AC02-06CH11357, the STFC (UK), the “RIKEN foreign research program”, the German BMBF (No. 05P12RDCIA, 05P12RDNUP and 05P12PKFNE), HIC for FAIR, the DFG cluster of excellence “Origin and Structure of the Universe” and DFG (Contract No. KR2326/2-1).

Appendix A. Considerations of γ-ray intensities and trigger conditions

To examine the plausibility of the structure proposed above the (10^+) state in ^{128}Cd (see Fig. 2c)) we estimate the intensities with which the different γ rays emitted in the decay of the (15^-) isomer are expected to be observed considering the experimental conditions such as coincidence time windows and detector thresholds as well as the half-lives of intermediate states and multipolarities of the involved transitions. The result of this estimation is compared to the experimentally determined intensities in Table 1. We start with an assessment of the probabilities for the different conversion electrons (CE), which are emitted in the decay of the ms isomer, to trigger the data acquisition based on their conversion coefficients. To take into account the time structure of the decay sequence we will apply the following two assumptions: i) In all cases in which either a 309 or a 203 keV CE is detected any further energy deposition related to transitions below the (10^+) isomer escapes observation due to the long half-life of the intermediate (10^+) state and the dead time of the data acquisition and ii) in case that two conversion electrons are emitted within a period of nanoseconds their energies are summed. On this basis we estimate probabilities of 9.7% for the 309 keV CE, 3.1% for the 203 keV CE, 69% for the 69 keV CE, 0.9% for the 238 keV CE and 4.9% for the sum of the 69 and 238 keV CEs, which corresponds to 307 keV. As mentioned before the detection probability for the 69 keV CE is drastically reduced due to the energy thresholds of the Si detectors leading to an effective trigger probability of 7.8% for the 69 keV CE. Note that hence the peak around 290 keV observed in the Si energy spectrum of Fig. 2b) contains contributions of both the 309 keV CE above and the sum of the 69 and 238 keV CEs below the (10^+) state. In this estimate the contribution of Compton electrons is neglected. Simulations in line with the ones presented in Ref. [7] estimate their contribution to be well below 5%. Summing all individual trigger probabilities shows that only every fourth decay of the newly identified ms isomer is observed at all. An illustration of the two main trigger modes, namely the 69 keV CE and the two components contributing to the peak around 290 keV, is given in Fig. 5. This figure shows the distributions of the time differences between the detection of the γ

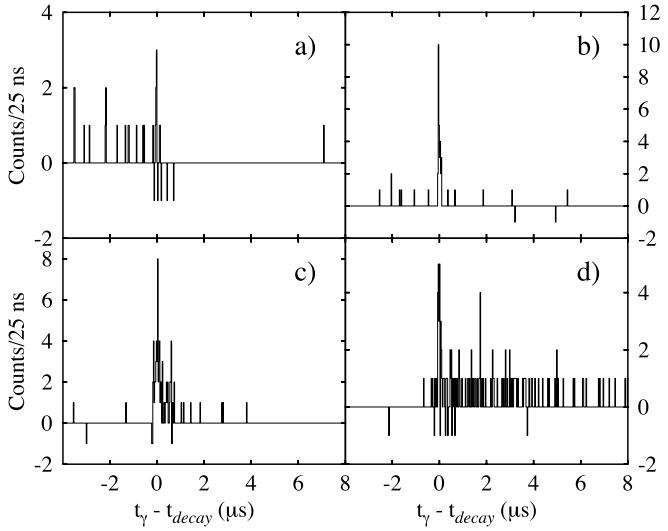

Fig. 5. Summed time difference distributions ($t_\gamma - t_{decay}$) for a) the 203, 309, 1060, and 1263 keV γ rays and a decay energy in the range labelled *I* in Fig. 2a), b) the same γ rays and a decay energy in the range labelled *II* in Fig. 2a), c) the 238, 440, 538, 646, and 785 keV γ rays and a decay energy in range *I* and d) the same γ rays as in c) and a decay energy in range *II*.

ray, t_γ, and the energy deposition in the Si detector, t_{decay}, for the two Si energy gates, *I* and *II*, indicated in Fig. 2b) and either the γ rays above or below the (10^+) isomer. Clearly the γ rays with 203, 309, 1060, and 1263 keV are emitted before the detection of a 69 keV CE in the Si detector (compare Fig. 5a)), while they are emitted in prompt coincidence with the 309 keV CE (see Fig. 5b)). For the 238, 440, 538, 646, and 785 keV γ rays observed in the decay of the (10^+) isomer, on the other hand, the time distribution with respect to the 69 keV CE nicely reflects the 270(7) ns half-life of the (5^-) state. Finally, Fig. 5d) shows that besides the short-lived component observed in Fig. 5c), the γ rays below the (10^+) isomer are also observed microseconds after the detection of an energy around 290 keV in the Si detector. This latter contribution stems from the 309 keV CE and reflects the half-life of $T_{1/2} = 3.56(6)$ μs of the (10^+) state. Note that the time range for the γ-ray detection before the Si trigger is in the present experiment limited to about 4 μs. Therefore the observed intensities of the γ rays above the (10^+) state are reduced by roughly a factor of two whenever the CE of a transition below this state triggers the data acquisition.

Combining all these pieces of information with respect to trigger probabilities and time constraints the expected intensities of the γ rays observed in Fig. 1 can now be estimated. The results of this estimate are compared to the experimentally determined values in Table 1. A good general agreement is observed providing indirect support for the assumptions made concerning the multipolarities of the 203 keV ($M1$) and 309 keV ($E3$) transitions.

References

[1] M. Górska, et al., Phys. Rev. Lett. 79 (1997) 2415.
[2] A. Jungclaus, et al., Phys. Rev. Lett. 99 (2007) 132501.
[3] B. Fogelberg, K. Heyde, J. Sau, Nucl. Phys. A 352 (1981) 157.
[4] B.S. Nara Singh, et al., Phys. Rev. Lett. 107 (2011) 172502.
[5] P.J. Davies, et al., Phys. Lett. B 767 (2017) 474.
[6] L. Cáceres, et al., Phys. Rev. C 79 (2009) 011301(R).
[7] J. Taprogge, et al., Phys. Lett. B 738 (2014) 223.
[8] T. Kubo, Nucl. Instrum. Methods B 204 (2003) 97.
[9] T. Ohnishi, et al., J. Phys. Soc. Jpn. 79 (2010) 073201.
[10] S. Nishimura, et al., Prog. Theor. Exp. Phys. 03C006 (2012).
[11] P.-A. Söderström, et al., Nucl. Instrum. Methods 317 (2013) 649.
[12] J. Eberth, et al., Nucl. Instrum. Methods A 369 (1996) 135.
[13] J. Simpson, Z. Phys. A 358 (1997) 139.
[14] B. Fogelberg, et al., in: Proc. Intern. Conf. Nuclear Data for Science and Technology, Mito (Saikon Publishing Co.), Tokyo, Japan, 1988, p. 837.
[15] G. Lorusso, et al., Phys. Rev. Lett. 114 (2015) 192501.
[16] R. Dunlop, et al., Phys. Rev. C 93 (2016) 062801(R).
[17] L. Coraggio, et al., Prog. Part. Nucl. Phys. 62 (2009) 135.
[18] H. Grawe, K. Langanke, G. Martínez-Pinedo, Rep. Prog. Phys. 70 (2007) 1525.
[19] A. Kankainen, et al., Phys. Rev. C 87 (2013) 024307.
[20] J. Taprogge, et al., Phys. Rev. Lett. 112 (2014) 132501.
[21] A. Scherillo, et al., Phys. Rev. C 70 (2004) 054318.
[22] G.S. Simpson, et al., J. Phys. Conf. Ser. 267 (2011) 012031.
[23] B.A. Brown, et al., OXBASH for Windows, MSU-NSCL report 1289, 2004.
[24] T.R. Rodríguez, J.L. Egido, A. Jungclaus, Phys. Lett. B 668 (2008) 410.
[25] J. Taprogge, et al., Phys. Rev. C 91 (2015) 054324.
[26] A. Jungclaus, et al., Phys. Rev. C. 94 (2016) 024303.
[27] J. Taprogge, et al., Eur. Phys. J. A 52 (2016) 347.
[28] H. Gausemel, et al., Phys. Rev. C 69 (2004) 054307.
[29] http://bricc.anu.edu.au/index.php.